FlowBO: A Flow Chemistry Bayesian Optimization Framework Benchmarked by Kinetic Models

Guihua Luo[a], Xilin Yang[a], Tingting Qi[a], Qilin Xu[a,b], Weike Su[a]*, and An Su[c]*

a. National Engineering Research Center for Process Development of Active Pharmaceutical Ingredients, Collaborative Innovation Center of Yangtze River Delta Region Green Pharmaceuticals, Zhejiang University of Technology, Hangzhou, 310014, P. R. China

b. School of Biological and Pharmaceutical Engineering, West Anhui University, Luan 237000, P. R. China

c. College of Chemical Engineering, Zhejiang University of Technology, Hangzhou 310014, P. R. China

Corresponding Authors

Prof. An Su

College of Chemical Engineering, Zhejiang University of Technology, Hangzhou 310014, P. R. China

Email: ansu@zjut.edu.cn

Prof. Weike Su

National Engineering Research Center for Process Development of Active Pharmaceutical Ingredients, Collaborative Innovation Center of Yangtze River Delta Region Green Pharmaceuticals, Zhejiang University of Technology, Hangzhou, 310014, P. R. China

Email: pharmlab@zjut.edu.cn

Abstract

The applications of flow chemistry (continuous flow reactions) in the synthesis of pharmaceuticals and fine chemicals require more advanced optimization algorithms to guide laboratory-scale and industry-scale optimization. Although several Bayesian Optimization (BO) frameworks have been developed, they are rarely equipped with state-of-the-art noise-handling acquisition functions and have not been benchmarked by multiple real-world continuous flow kinetic models. In this study, we developed FlowBO for flow chemistry, equipped with the recently-developed MOO algorithm qNEHVI that can better handle experimental noise and make parallel recommendations. Also, five kinetic models built from experimental results, including four series reactions, were used as benchmarks for FlowBO and two other recognized BO frameworks. The results show that FlowBO outperforms in all four series reaction cases with optimization results >99.9% for conversion and selectivity. At the same time, FlowBO offers a range of optimum advantages with a wide choice of temperature, residence time, and reactant concentration, facilitating process optimization for subsequent steps (i.e. separation).

Keywords

Bayesian optimization, flow chemistry, continuous flow, self-optimization, multi-objective optimization, kinetic models, acquisition function, machine learning

Introduction

Continuous flow chemistry is flourishing in the pharmaceutical industry due to its precise control of reaction parameters, high degree of automation, ease of integration, and safety of the reaction[1]. Optimization of flow chemistry reaction parameters (residence time, temperature, pressure, reactant concentration, etc.) is important to improve the conversion and selectivity of target products and control experimental costs. How to obtain the optimal reaction parameters used to be a complex and expensive problem. Traditionally, chemists optimized reaction conditions based on their own expertise and relevant literature, which was prone to human bias and required a lot of time to screen reaction parameters. In addition, only a limited number of experiments could be performed due to time and material budget constraints. In recent years, chemists have applied optimization algorithms to develop more efficient optimization methods[2]., including determining the optimal conditions for industrial processes[3], predicting reaction paths[4, 5], and finding derivatives of specific molecules[6]. Design of Experiments (DOE), a local optimization algorithm, has been found to work well in many areas of chemical synthesis[7, 8, 9]. However, the number of experiments designed by DOE increases exponentially with the number of factors increases. In addition, the locally optimal solutions are only superior to neighboring solutions and are not guaranteed to be optimal, making DOE less suitable for optimizing chemical reactions with more than two variables[10]. Therefore, it is important to find a non-convex global optimization method to optimize expensive objectives.

Bayesian optimization (BO) is a sequential model-based approach that was initially developed to find optimal solutions to black box functions[11-13]. BO has two major components. The first component is the surrogate model, which is trained using the results of previous evaluations while making predictions for the unevaluated experiments. The second component is the acquisition function, which verifies the predictions of the agent model by evaluating the results, balancing exploitation (evaluating the optimal part of the solution) and exploration (evaluating the part with

high uncertainty) before selecting the next evaluation point to validate its conjecture. Various models have been proposed as surrogate functions, including Random Forests[14], Gaussian Processes[11, 15], and Bayesian Neural Networks[16]. BO can be applied to a wide range of search spaces and recommend and process multiple experiments in parallel, which makes it well-suited for the optimization of chemical reactions[17-19]. Deshwal et al. applied BO to the screening of nanoporous materials, comparing it systematically with evolutionary search and one-time supervised machine learning[20]. Doyle group optimized the Mitsunobu and defluorination oxidation reactions and found BO outperformed human decision-making in terms of average optimization efficiency and consistency[3]. Lapkin group developed the Summit platform, which compared seven different optimization strategies and demonstrated the efficiency of BO[21].

When optimizing chemical reactions, one often encounters the difficulty of optimizing not only one but multiple objectives. For example, selectivity and conversion in a chemical reaction are competing objectives, and it is difficult to find a point where both are maximized. Optimization of one of the objectives means a detrimental effect on the other, and the best solution for such competing objectives is usually to find a compromise between the two. Many studies have reported algorithms for multi-objective optimization (MOO) such as Thompson Sampling Efficient Multi-objective (TS-EMO)[22, 23], Expected Hypervolume Improvement (EHVI)[24], and Noisy Expected Hypervolume Improvement (NEHVI)[25]. Some studies have applied these algorithms to chemical reactions. Lapkin et al. applied TSEMO to the multi-objective optimization of the SnAr reaction optimizing space-time yield (STY) and E factor (ratio of total waste to product), and an N-benzylation reaction to optimize STY and impurity yield[26]. Vlachos et al. developed an open-source BO framework, NEXTorch, and applied it to optimize the conversion of fructose to 5-hydroxymethylfurfural[27].

Although there are many BO algorithms for MOO, most methods do not take into account the effect of noise on observations[25]. For example, in the laboratory, environmental factors such as temperature and air pressure, as well as instrument

stability and other errors, can have an impact on observations, and a good noise-handling method can significantly improve the optimization performance. In addition, few existing BO frameworks have been benchmarked[21] by kinetic modeling, an recognized method for optimizing flow chemistry experiments. In this study, we presented FlowBO, a BO framework specifically designed for flow chemistry. FlowBO is equipped with a recently developed noise-handling acquisition function. It also supports parallel recommendations of experiments and offers both single-objective optimization (SOO) and MOO. In addition, we simulated the experimental results with five kinetic models, which also serve as a benchmark to compare FlowBO with other existing BO frameworks.

Methods

FlowBO, a flow chemistry Bayesian optimization (BO) framework. FlowBO was implemented in a modular way based on the open-source framework BoTorch[28]. The flowchart of FlowBO is shown in Figure 1. The user first determines the relevant parameters (range of decision variables, number of iterations, etc.) and optimization objectives. The initial experimental data collected by the LHS, an efficient method for sampling from multiple distributions[29], is used to initialize FlowBO by training the surrogate model for the first time. After the trade-off between exploration and development, the acquisition function will propose new experimental points for new experiments. And then the experimental dataset will be extended and the surrogate model will be updated. Subsequently, the process continues iteratively until the maximum number of iterations is reached. Finally, the visualization module is invoked to present the experimental results in graphical form.
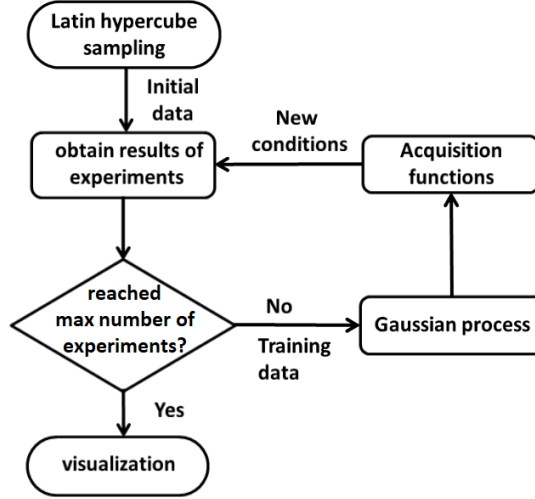
Figure 1. Flow chart of FlowBO multi-objective optimization

Surrogate model: Gaussian Process (GP). The Gaussian Process is known to perform well at locating optimal solutions, generating accurate surrogate models, and effectively using information gathered from a priori experiments[11]. A common class of covariance functions is the Mat*é*rn class[30].

$$\mathbf{k(x, x'):} = \sigma_f^2 \frac{2^{1-v}}{\Gamma(v)} (\sqrt{2}vr)^v K_v(\sqrt{2}vr) \tag{1}$$

Where σ_f^2 is the output variance，r is a weighted Euclidean distance, v is non-negative parameters, K_v is the modified Bessel function, Γ is the gamma function

Acquisition functions and Multi-objective optimization (MOO). The new sampling points obtained from the acquisition function are used to plot the Pareto front. The Pareto front is a solution to a multi-objective optimization problem that shows the best compromise between competing objectives. Expected hypervolume improvement (EHVI) [31] is an extension of the expected improvement (EI)[32] acquisition function to the MOO setup. qEHVI [Eq. (2)] and Noisy expected hypervolume improvement (NEHVI) [Eq. (3)] are a new MOO algorithm based on EHVI. qEHVI is an exact computation of the joint EHVI of q new candidate points, whose limitations are the assumption of noiseless observations and limited use in high-dimensional target space. NEHVI is a hypervolume-maximizing BO in noisy and noiseless environments that performs well in large-batch environments and is

capable of evaluating noisy objectives in a highly parallel fashion[25].

$$\alpha_{qEHVI}(\mathcal{X}_{cand}) = \mathbb{E}[HVI(f(\mathcal{X}_{cand}))] \qquad (2)$$

$$\hat{\alpha}_{qNEHVI}(\mathcal{X}_{cand}) = \frac{1}{N}\sum_{t=1}^{N} HVI(\tilde{f}(\mathcal{X}_{cand})|P_t) \qquad (3)$$

Where $\mathcal{X}_{cand}$ is the candidate sample, HVI is the hypervolume improvement, P_t is the pareto frontier, f is the Black-box objective function, $\tilde{f}$ is the sampling function, N is the number of samples.

TSEMO is an algorithm for approximating Pareto sets with a small number of functionally-valued approximations. It extends the Thompson sampling (TS) method from multi-armed bandit communities to continuous multi-objective optimization. It is defined as:

$$\text{minimize}_{x\in\mathcal{X}\subseteq\mathbb{R}^d}\boldsymbol{G}(\mathbf{x}) = [g_1(\mathbf{x}), g_2(\mathbf{x}), \ ..., g_m(\mathbf{x})] \qquad (4)$$

Where $\mathcal{X}$ is the design space, $\mathbf{x}$ is the decision vector and G is a vector of m scalar objectives $g_i(\mathbf{x})$ to be minimized.

Single-objective optimization(SOO). qNEI (noisy expected improvement)[33] is an extension of the EI and is ideal for high noise settings. Its equation is:

$$\text{qNEI}(x;\mathcal{D}) = \mathbb{E}[(\max g(\xi) - \max g(\xi_{obs}))_+ |\mathcal{D}] \qquad (5)$$

Where $\mathcal{D}$ is the data collected, ξ is a hyperparameter, g is the Black-box objective function.

Generation of experimental data. Since our group has been developing kinetic models extensively over the last five years, we have accumulated a number of kinetic models of flow chemistry reactions that are based on and validated by a large number of experimental results[34-36]. Therefore, in this study, we used four of our models as well as one model from the Jensen group[37] to simulate the experimental results. Under the new reaction conditions recommended by the acquisition function, the conversion and selectivity of these experiments are calculated by solving the integral of the kinetic models by the SciPy package (https://scipy.org/, accessed February 8th, 2023).

On the other hand, our FlowBO is also suitable for situations where no kinetic model is available and manual experiments must be performed. In this case, after outputting a new set of experimental conditions, the FlowBO framework can pause

and wait for the user to input new experimental results.

Results

We performed the multi-objective optimization (MOO) of conversion and selectivity and the single-objective (SOO) optimization of yield for each of the five cases to demonstrate the basic process and functionality of FlowBO. The kinetic model of each reaction was used as an objective function to calculate the experimental results. An error of ±3% was added to the calculated concentrations to simulate the error that would occur under real experiments. In addition, to further validate the reliability of FlowBO in MOO, we compared FlowBO with two recognized BO frameworks including NEXTorch[27] and Summit-TSEMO (TSEMO model implemented in the Summit framework), with the same number of LHS samples and BO iterations. Furthermore, FlowBO has a visualization module to plot the Pareto front of the optimization results and a time module to calculate the optimization time.

For MOO, the procedure shown in Figure 1 was followed for each case, with an initial 15 instances of experimental conditions obtained through LHS, followed by 15 iterations of BO with 4 parallel recommendations per iteration. The same procedure was repeated on NEXTorch and Summit-TSEMO, using the same number of initial experiments and iterations. The three optimal results and their corresponding experimental conditions suggested by each platform were presented for each case.

To demonstrate the advantage of MOO over SOO, we combined conversion and selectivity into yield and performed SOO using FlowBO with qNEI as the acquisition function, using the same four decision variables as for MOO. Unlike the MOO strategy proposed in Figure 1, SOO did not require LHS but started with a random set of experimental conditions, and 20 iterations were performed with 1 recommendation per iteration. Although the optimization target for SOO was the yield, the corresponding conversion and selectivity were computed to compare with the MOOs.

A full record of the optimization data for the four models, including the value of decision variables and optimization objectives, was provided in the Supplemental

Information (S.I.).

Case 1: Grignard Addition to Esters

The kinetic model of Case 1 was developed by the Jensen group[37] (Scheme 1). The addition reaction of Phthalide **1** and 4-fluorophenylmagnesium bromide **2** produces the desired product, the mono-addition product **4,** and the by-product di-addition product **5**. The kinetic equation was established assuming that ketone 4 was in a pseudo-steady state.
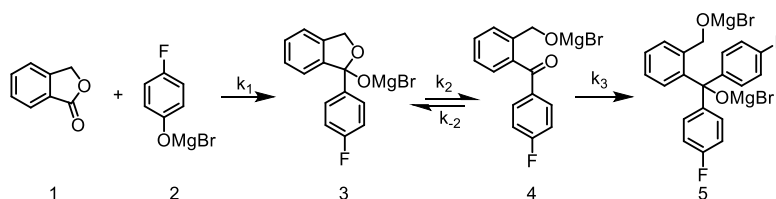
Scheme 1. Grignard Addition to Esters

Equations 6-10 outlined four differential equations of reaction kinetics containing four reaction constants k_i. The decision variables and their ranges were temperature (-30-0°C), residence time (1-3600s), the concentration of Phthalide **1** (0.01-1 mol/l), and the concentration of 4-fluorophenylmagnesium bromide **2** concentration (0.01-1 mol/l). The MOO objectives were the conversion and selectivity of the target product **4** among the four decision variables.

$$\frac{d[C_1]}{d\tau} = -k_1[C_1][C_2] \tag{6}$$

$$\frac{d[C_2]}{d\tau} = -k_1[C_1][C_2] - k_c[C_3][C_2] \tag{7}$$

$$\frac{d[C_3]}{d\tau} = k_1[C_1][C_2] - k_c[C_3][C_2] \tag{8}$$

$$\frac{d[C_5]}{d\tau} = k_c[C_3][C_2] \tag{9}$$

$$k_c = \frac{k_3 k_2}{k_{-2}} \tag{10}$$

All three MOO models showed similar Pareto fronts (Figure 2). However, only FlowBO and NEXTorch found conditions where both conversion and selectivity were higher than 99.9% (Table 1). In addition, although the Top-3 suggestions of FlowBO and NEXTorch gave similar optimization results, FlowBO provided a more flexible choice of decision variables. For example, the second optimal result of FlowBO

(Iteration 59) is significantly different from the first optimal result (Iteration 10) in temperature, residence time, and concentrations. In contrast, no significant differences were observed for the first two optimal results of NEXTorch, except for residence time. One possible reason was that FlowBO has a higher propensity to explore (preferring to search in unexplored regions) since the complete optimization record shows that FlowBO and TSEMO have wider search ranges than NEXTorch for all four decision variables (Figure S1 and S2).

In terms of search efficiency, FlowBO achieved a Top-1 result with the smallest number of iterations (10) compared to NEXTorch (55) and Summit-TSEMO (34) (Table 1). The computational time for the whole optimization is shown at the end of the results section, together with the computational time of the other cases.
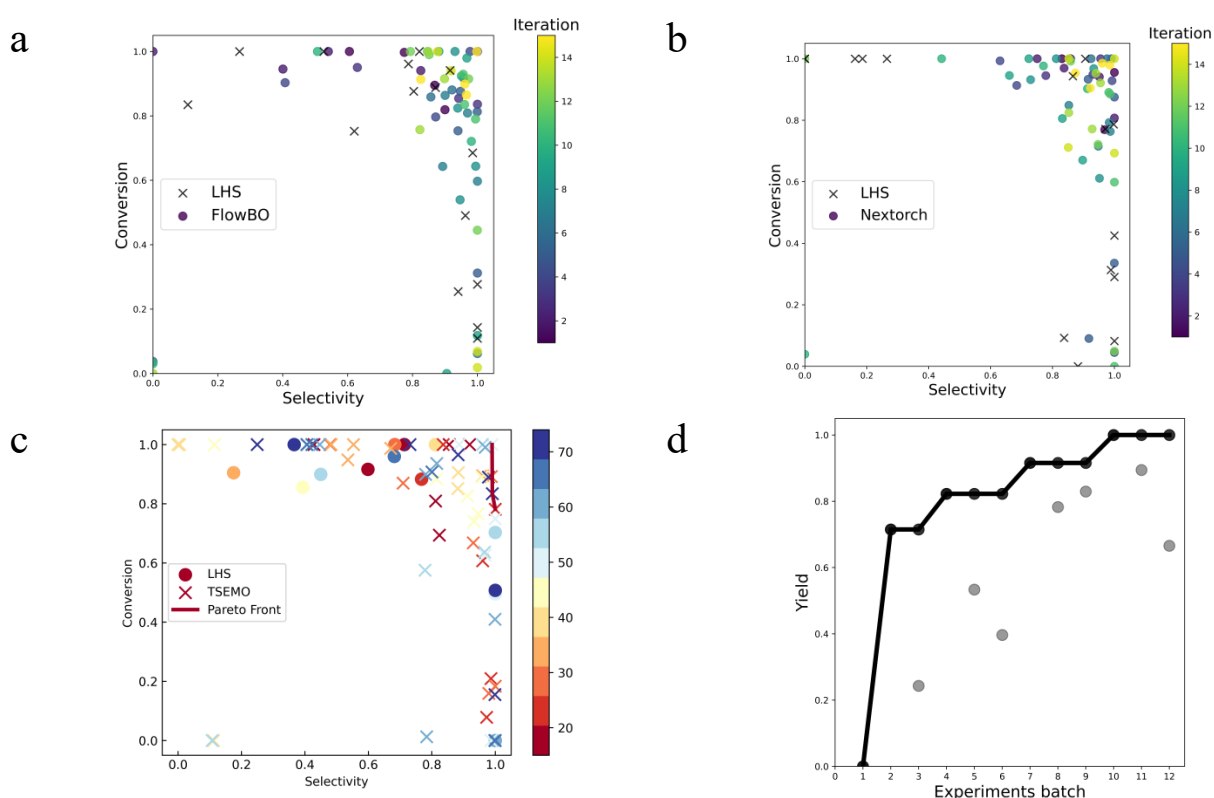

Figure 2. Case 1 optimization results of MOO using a) FlowBO, b) NEXTorch, and c) Summit-TSEMO, with the color bar showing number of iterations, and of SOO using d) FlowBO with black solid lines showing the cumulative best-observed yield and grey dots showing other experiments.

Table 1. Decision variables and objectives values of Case 1, with three best conditions recommended by FlowBO (multiple), NEXTorch, Summit-TSEMO, and FlowBO (single).

Suggested by	Iteration round	Residence time (s)	Temperature (°C)	Conc. of 1 (mol/l)	Conc. of 2 (mol/l)	Conversion	Selectivity
FlowBO (MOO)	10	829.0	-27.98	0.7088	0.9588	0.9999	0.9999
	59	1649	-18.76	0.5676	0.5800	0.9999	0.9980
	14	1199	-30.00	0.5281	0.8917	0.9999	0.9772
NEXTorch	55	967.1	-30	0.5853	0.7597	0.9999	0.9999
	20	1307	-30	0.5262	0.7903	0.9999	0.9902
	21	1001	-30	0.541	0.6823	0.9999	0.9761
Summit-TSEMO	34	1182	-1.761	0.1528	0.1310	0.9999	0.9898
	42	1414	-30.00	0.3939	0.3811	0.9999	0.9595
	47	2607	-22.45	0.2329	0.2857	0.9909	0.9684
FlowBO (SOO)	10	2882	-30.00	0.9999	0.997	0.9999	0.9999
	7	2255	-19.73	0.8125	0.8283	0.9420	0.9720
	11	3600	-18.43	0.9999	0.9999	0.9505	0.9407

On the other hand, FlowBO-SOO output much higher residence times and concentrations than MOO at optimal values of the objectives similar to MOO. Interestingly, like all MOOs, FlowBO-SOO also found that the lowest temperature in the limit range (-30°C) favors higher selectivity.

Case 2. Condensation amidation of piperazine with benzoic acid

The kinetic model of Case 2 developed by our group in 2021[36] is the acylation of benzoic acid **6**, piperazine **7**, and 2-(7-azabenzotriazole)-N,N,N',N'-tetramethyluronium hexafluorophosphate (HATU) to give the target product 1-benzoylpiperazine **8** and the by-product N,N'-dibenzoylpiperazine **9**.
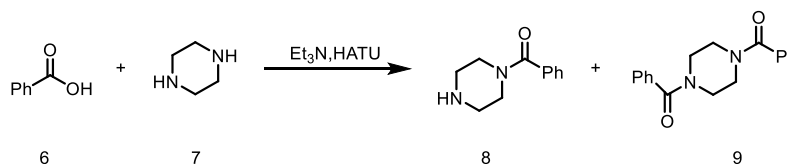
Scheme 2. condensation amidation of piperazine with benzoic acid

Equations 11-12 have 2 differential equations containing reaction constants k_1 and k_2. The decision variables and their ranges are temperature (-10-70 °C), residence

time (1-100 s), the concentration of benzoic acid **6** (10-120 mmol/l), the concentration of HAUT (10-120 mmol/l), and concentration of piperazine **7** (10-120 mmol/l). Different from Case 1, Case 2 has three concentrations in the decision variables.

$$r_1 = k_1 C_6 C_{HAUT}^{0.61} C_7^{0.45} \qquad (11)$$

$$r_2 = k_2 C_6 C_{HAUT}^{0.61} C_7^{0.45} \qquad (12)$$

In Case 2, the selectivity at the optimal point of the three MOO outputs is relatively lower than in Case 1 (Table 2), which indicates that it is more difficult to compromise conversion and selectivity in this case. Figure 3 and Table 2 show that a further increase in selectivity from the current optimal point leads to a dramatic decrease in conversion. Furthermore, NEXTorch shows a narrower Pareto Front than FlowBO and TSEMO, which again infers NEXTorch is more inclined to exploitation compared to FlowBO and TSEMO. However, in this case, NEXTorch's adherence to exploitation leads to slightly better optimization results than FlowBO (conversion 0.9999 vs 0.9997 and selectivity 0.9705 vs. 0.9684).
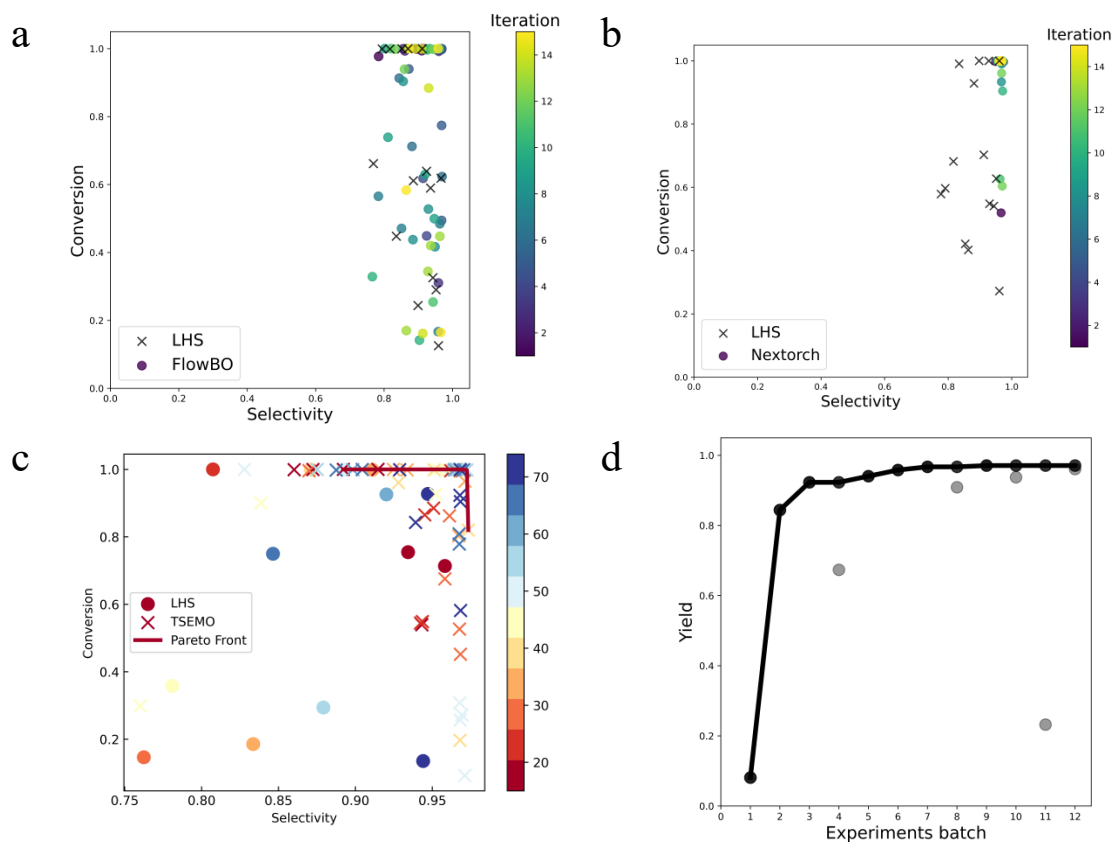

Figure 3. Case 2 optimization results of MOO using a) FlowBO, b) NEXTorch, and c) Summit-TSEMO, with the color bar showing number of iterations, and of SOO using d) FlowBO with black solid lines showing the cumulative best-observed yield and grey dots showing other

Table 2. Decision variables and objectives values of Case 2, with three best conditions recommended by FlowBO (multiple), NEXTorch, Summit-TSEMO, and FlowBO (single).

Suggested by	Iteration round	Residence time (s)	T (℃)	Conc. 6 (mmol/l)	Conc. HAUT (mmol/l)	Conc. 7 (mmol/l)	Conversion	Selectivity
FlowBO (MOO)	20	100.0	-10.00	50.25	120.0	120.0	0.9997	0.9687
	10	49.46	-10.00	40.89	119.6	88.26	0.9994	0.9684
	13	100.0	-10.00	116.5	120.0	120.0	0.9973	0.9679
NEXTorch	14	41.55	-8.852	10.00	95.91	99.94	0.9968	0.9744
	36	58.57	-10.00	10.00	83.63	62.18	0.9999	0.9705
	30	43.21	-10.00	23.87	86.75	120.0	0.9999	0.9704
Summit-TSEMO	43	47.24	-10.00	10.03	120.0	88.82	0.9984	0.9724
	51	93.49	-9.998	17.76	49.45	120.0	0.9991	0.9705
	41	28.48	-10.00	62.63	105.1	118.9	0.9994	0.9684
FlowBO (SOO)	9	100.0	-10.00	10.00	66.48	43.61	0.9999	0.9708
	7	51.03	-10.00	10.00	86.61	86.93	0.9999	0.9672
	19	10.35	-10.00	10.00	120.0	120.0	0.9999	0.9666
Manual Optimization	/	50.00	0	100.0	100.0	100.0	0.9900	0.9520

Surprisingly, in this case, FlowBO-SOO outperformed FlowBO-MOO in terms of conversion and selectivity. A possible reason for this is the simplicity of this one-step reaction compared to the three-step reaction in Case 1. On the other hand, another comparison from Case 2 is between the MOO results and the manual optimization results reported in the literature. Table 2 shows that by using lower temperatures, all MOO models achieved higher conversions and selectivity than the manual optimization.

Case 3, the continuous flow monoacylation reaction of o-phenylenediamine and benzoic anhydride

The kinetic model of Case 3, developed by our group in 2021[35], is the acylation reaction of o-phenylenediamine **10** and benzoic anhydride **11**, the target product being the monoacylation product N-(2-aminophenyl)benzamide **12** and the by-product being the diacylation product N-(2-aminophenyl)benzamide **13** (Scheme 3).
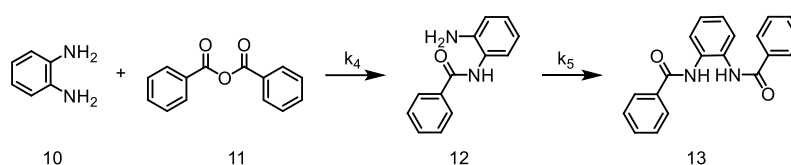
Scheme 3. Continuous flow monoacylation reaction of o-phenylenediamine and benzoic anhydride

Equations 13-16 are the four differential equations containing reaction constants k_4 and k_5. The decision variables including residence time (1-1000 s), temperature (0-120 °C), concentration of o-phenylenediamine 10 (0.01-0.3 mol/l), and benzoic anhydride 11 (0.01-0.3 mol/l).

$$\frac{d[C_{10}]}{d\tau} = -k_4[C_{10}][C_{11}] \tag{13}$$

$$\frac{d[C_{11}]}{d\tau} = -k_4[C_{10}][C_{11}] - k_5[C_{11}][C_{12}] \tag{14}$$

$$\frac{d[C_{12}]}{d\tau} = k_4[C_{10}][C_{11}] - k_5[C_{11}][C_{12}] \tag{15}$$

$$\frac{d[C_{13}]}{d\tau} = k_5[C_{11}][C_{12}] \tag{16}$$

The results in Table 3 show that all four BO models outperformed the human optimization, but only FlowBO-MOO and FlowBO-SOO had conversions and selectivity higher than 99.9%. However, FlowBO-SOO had a significantly longer residence time than FlowBO-MOO in achieving these results (1000s versus 267.1s)

Regarding Pareto Fronts (Figure 4), FlowBO and Summit-TSEMO reached both the region of higher conversion and lower selectivity (topmost horizontal line) and the region of lower conversion and higher selectivity (the rightmost vertical line), while NEXTorch only reached the latter. The complete optimization record (Figure S6) shows NEXTorch took many iterations at a concentration of 0.010 mol/l for **11**, while FlowBO had more exploration at **11** and found three optimal results at three different concentrations (Table 3). On the other hand, TSEMO had a lower search coverage of concentrations than FlowBO, which led to suboptimal results in the conversion.
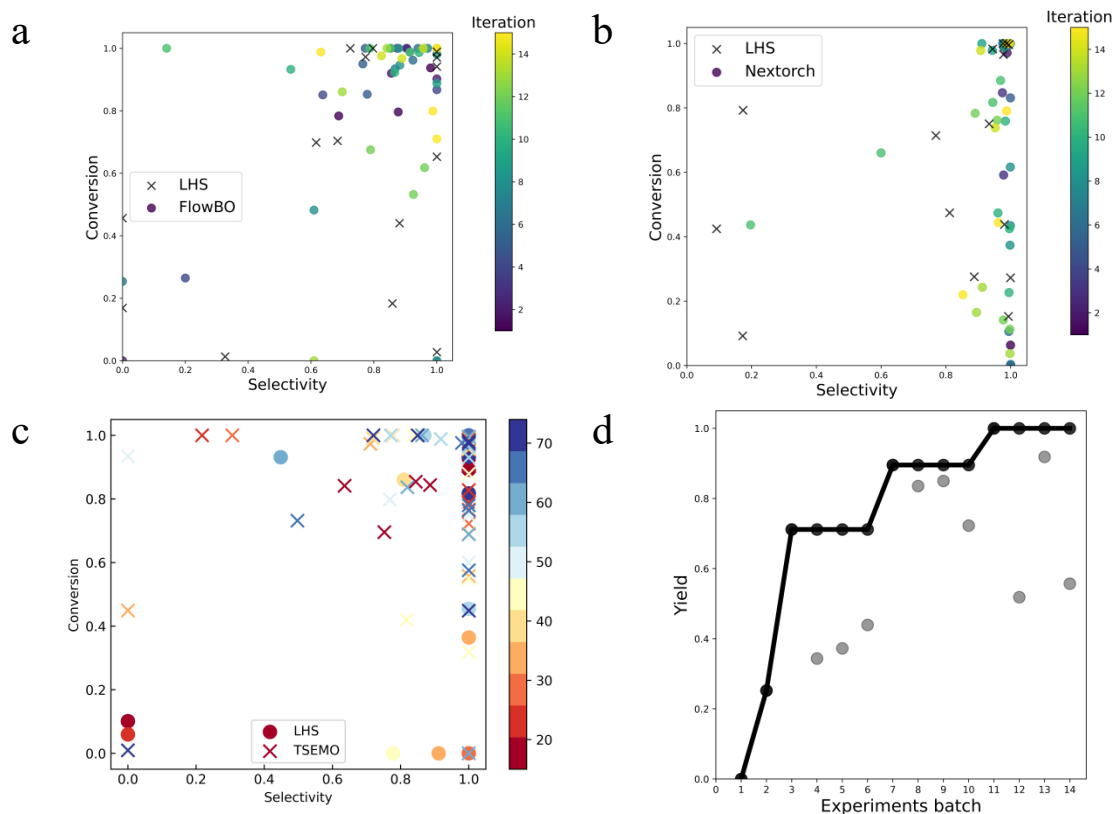
Figure 4. Case 3 optimization results of MOO using a) FlowBO, b) NEXTorch, and c) Summit-TSEMO, with the color bar showing number of iterations, and of SOO using d) FlowBO with black solid lines showing the cumulative best-observed yield and grey dots showing other experiments.

Table 3. Decision variables and objectives values of Case 3, with three best conditions recommended by FlowBO (multiple), NEXTorch, Summit-TSEMO, and FlowBO (single).

Suggested by	Iteration round	Residence time(s)	Temperature (°C)	Conc. 10 (mol/l)	Conc. 11 (mol/l)	Conversion	Selectivity
FlowBO (MOO)	6	267.1	47.74	0.3000	0.1254	0.9999	0.9999
	10	158.9	101.0	0.2541	0.2021	0.9999	0.9999
	11	408.3	77.4	0.2903	0.0608	0.9999	0.9999
NEXTorch	9	442.6	55.83	0.3000	0.0100	0.9999	0.9988
	16	914.7	79.91	0.3000	0.0100	0.9999	0.9987
	12	940.3	43.22	0.2330	0.0100	0.9999	0.9986
Summit-TSEMO	54	591.1	120	0.2732	0.1795	0.9948	0.9999
	58	839.3	69.86	0.2309	0.1849	0.9947	0.9999
	38	1000	120	0.2175	0.1544	0.9939	0.9999
FlowBO (SOO)	11	1000	29.79	0.3	0.2614	0.9999	0.9999
	15	1000	116.1	0.3	0.1523	0.9999	0.9999
	13	1000	55.07	0.2249	0.3	0.9477	0.9692
Manual experimentation	/	336.0	70.00	0.1800	0.1000	0.9810	0.9760

Case 4, continuous flow monoacylation reaction of m-phenylenediamine and benzoic anhydride

The model of Case 4 was the acylation reaction of m-phenylenediamine **14** and benzoic anhydride **11**, the target product being the monoacylation product N-(3-aminophenyl)benzamide **15**, and the by-product being the bisacylation product N, N'-dibenzoyl-1,3-benzenediamine **16** (Scheme 4)[34].
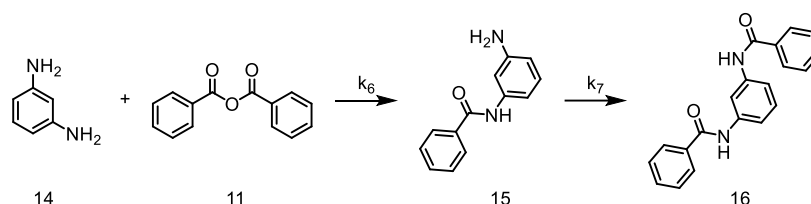
Scheme 4. Continuous flow monoacylation reaction of m-phenylenediamine and benzoic anhydride

Equations 17-20 had four differential equations containing two reaction constants k_6 and k_7. The decision variables and ranges were resistance time (1-1000 s), temperature (30-130 °C), and the concentration of m-phenylenediamine 14 (0.01-0.4 mol/l) and benzoic anhydride 11 (0.01-0.2 mol/l).

$$\frac{d[C_{14}]}{d\tau} = -k_6[\,C_{14}][C_{11}] \tag{17}$$

$$\frac{d[C_{11}]}{d\tau} = -k_6[\,C_{14}][C_{11}] - k_7[\,C_{11}][C_{15}] \tag{18}$$

$$\frac{d[C_{15}]}{d\tau} = k_6[\,C_{14}][C_{11}] - k_7[\,C_{11}][\,C_{15}] \tag{19}$$

$$\frac{d[C_{16}]}{d\tau} = k_7[\,C_{11}][C_{15}] \tag{20}$$

In this case, all MOO and SOO models, except TSEMO, found their optimal data points with conversions and selectivity above 99.9%. For models with more than three sets of experimental conditions leading to this optimal result, only the three sets with the lowest number of iterations are shown in Table 4, while the rest are shown in Table S4. However, the optimal points of FlowBO-MOO provided a more flexible choice of temperature (from 57.25 to 120.0℃) and residence time (from 91.85s to 1000s), while temperatures above 100 ℃ and residence times below 500 s were not seen in the optimum results of NEXTorch (Table S4). In addition, although FlowBO-MOO and NEXTorch showed similar Pareto Front patterns, their

optimization records show that FlowBO-MOO explored a wider range of residence times and temperatures (Figure S7).
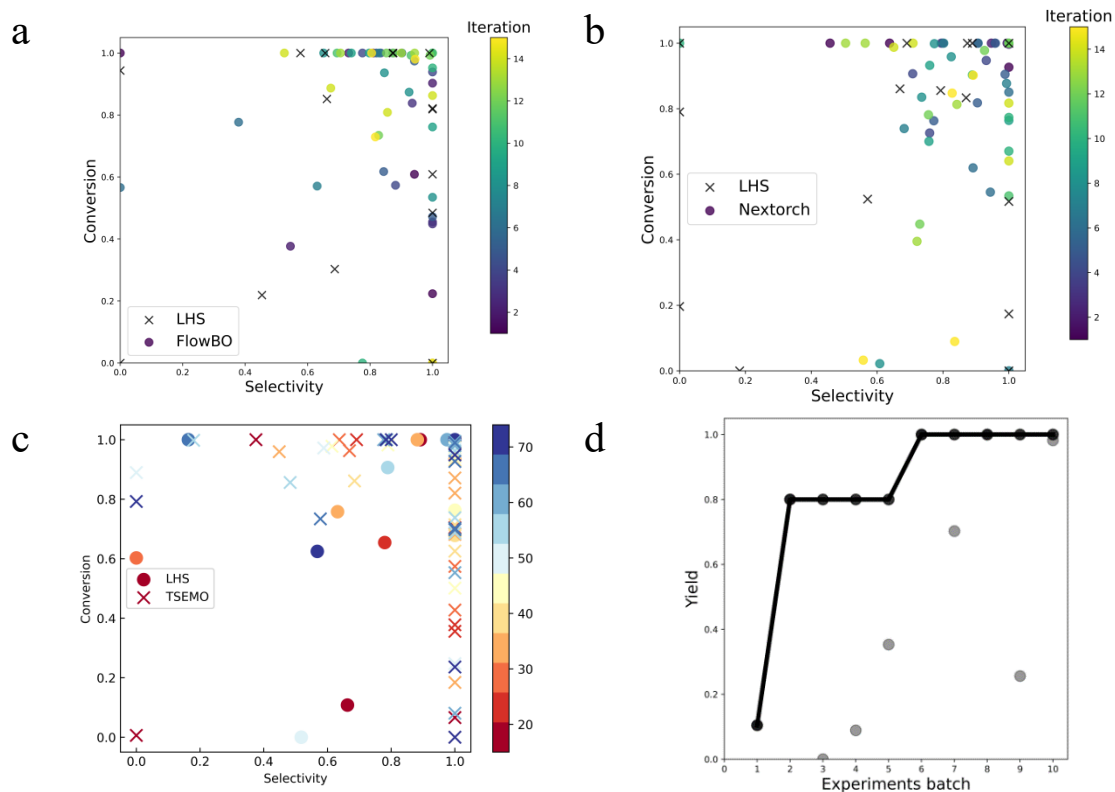

Figure 5. Case 4 optimization results of MOO using a) FlowBO, b) NEXTorch, and c) Summit-TSEMO, with the color bar showing number of iterations, and of SOO using d) FlowBO with black solid lines showing the cumulative best-observed yield and grey dots showing other experiments.

Table 4. Decision variables and objectives values of Case 4, with three best conditions recommended by FlowBO (multiple), NEXTorch, Summit-TSEMO, and FlowBO (single).

Suggested by	Iteration round	Residence time(s)	Temperature (℃)	Conc. 14 (mol/l)	Conc. 11 (mol/l)	Conversion	Selectivity
FlowBO (MOO)	7	825.1	57.25	0.2494	0.1133	0.9999	0.9999
	27	811.7	105.8	0.3718	0.2	0.9999	0.9999
	33	1000	61.57	0.3378	0.1754	0.9999	0.9999
NEXTorch	1	783.24	74.68	0.3625	0.1176	0.9999	0.9999
	11	758.0	72.80	0.2310	0.2000	0.9999	0.9999
	12	765.3	99.33	0.4000	0.146	0.9999	0.9999
Summit-TSEMO	46	725.4	106.5	0.3125	0.1638	0.9943	0.9999
	6	791.8	79.12	0.3381	0.1353	0.993	0.9999
	54	997.7	75.82	0.3999	0.0905	0.9896	0.9999
FlowBO (SOO)	6	692.1	107.1	0.32	0.08	0.9999	0.9999
	8	489.3	120	0.33	0.04	0.9999	0.9999
	17	905.7	103.8	0.37	0.14	0.9999	0.9999
Manual experimentation	/	528.0	70.00	0.3000	0.1000	0.9840	0.9690

Case 5, continuous flow monoacylation reaction of p-phenylenediamine and benzoic anhydride

The kinetic model (Case 5) was the acylation reaction of p-phenylenediamine 17 and benzoic anhydride **11**, the target product was the monoacylation product N-(4-aminophenyl)-benzamide **18**, and the by-product was the diacylation product N,N'-dibenzoyl-1,4-benzenediamine **19** (Scheme 5)[35].
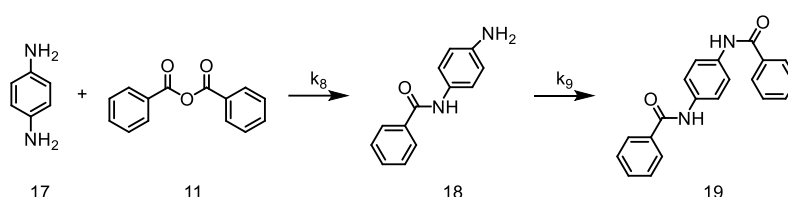
Case 5. Continuous flow monoacylation reaction of p-phenylenediamine and benzoic anhydride

Equations 21-24 outline the kinetic equation for Scenario 4, which consists of four differential equations containing two reaction constants k_8 and k_9 with a decision variable of resistance time (1-200 s), temperature (0-120 °C), the concentration of p-phenylenediamine 17 (0.01-0.3 mol/l) and benzoic anhydride 11 (0.01-0.3 mol/l).

$$\frac{\mathrm{d}[C_{17}]}{d\tau} = -k_8[\,C_{17}][C_{11}] \tag{21}$$

$$\frac{\mathrm{d}[C_{11}]}{d\tau} = -k_8[\,C_{17}][C_{11}] - k_9[\,C_{11}][C_{18}] \tag{22}$$

$$\frac{\mathrm{d}[C_{18}]}{d\tau} = k_8[\,C_{17}][C_{11}] - k_9[\,C_{11}][\,C_{18}] \tag{23}$$

$$\frac{\mathrm{d}[C_{19}]}{d\tau} = k_9[\,C_{11}][C_{18}] \tag{24}$$

Only the MOO and SOO of FlowBO achieved more than 99.9% in both conversion and selectivity (Table 5). The selectivity was lower for NEXTorch, while the conversion was lower for TSEMO. Other observations were similar to Case 4: NEXTorch's Pareto Front had a narrower coverage (Figure 6), while FlowBO's decision variables were more flexible (Table 5). The FlowBO-SOO required a higher temperature. All MOO and SOO results were better than the manual optimization results.
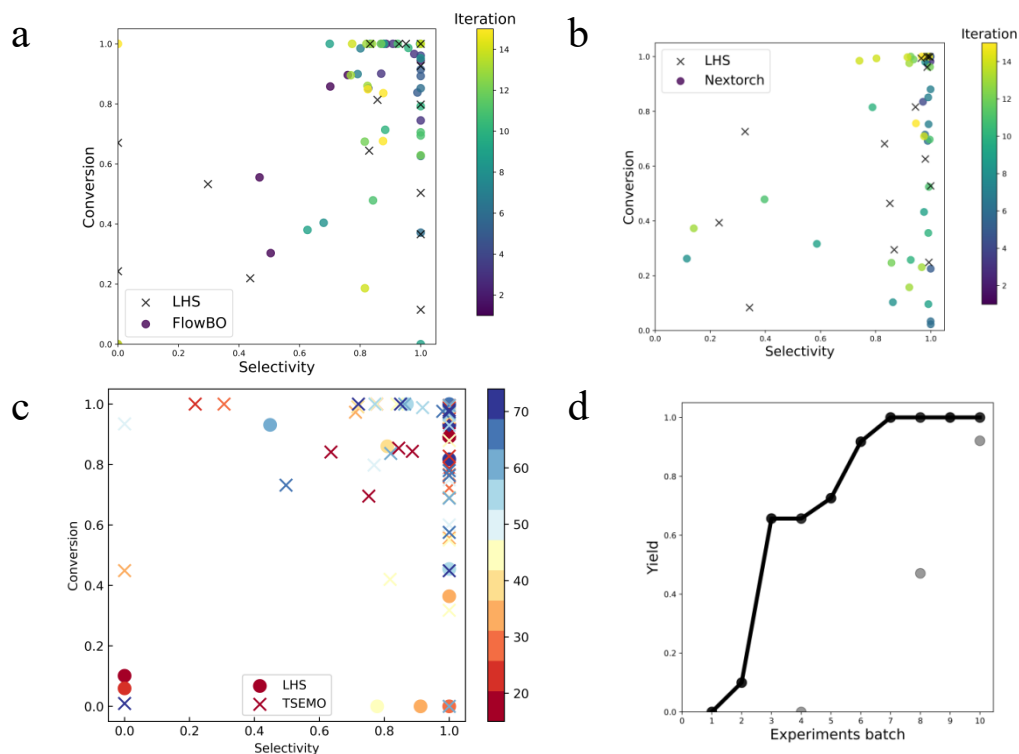
Figure 6. Case 5 optimization results of MOO using a) FlowBO, b) NEXTorch, and c) Summit-TSEMO, with the color bar showing number of iterations, and of SOO using d) FlowBO with black solid lines showing the cumulative best-observed yield and grey dots showing other experiments.

Table 5. Decision variables and objectives values of Case 5, with three best conditions recommended by FlowBO (multiple), NEXTorch, Summit-TSEMO, and FlowBO (single).

Suggested by	Iteration number	Residence time(s)	Temperature (°C)	Conc. of 17 (mol/l)	Conc. of 11(mol/l)	Conversion	Selectivity
FlowBO (MOO)	5	114.7	97.02	0.2168	0.1114	0.9999	0.9999
	8	133.4	63.65	0.2626	0.2388	0.9999	0.9999
	13	74.49	120	0.3	0.1244	0.9999	0.9999
NEXTorch	1	119.6	55.83	0.2384	0.0748	0.9999	0.9924
	11	193.1	34.55	0.261	0.01	0.9999	0.9993
	12	109	76.36	0.3	0.01	0.9999	0.9993
Summit-TSEMO	14	190.6	120	0.2238	0.2421	0.9961	0.9999
	46	155.9	84.45	0.3	0.1971	0.9952	0.9999
	34	142.9	101.5	0.2529	0.172	0.9945	0.9999
FlowBO (SOO)	7	52.22	112.6	0.1538	0.0276	0.9999	0.9999
	9	61.71	98.59	0.0756	0.01	0.9999	0.9999
	12	83.31	112	0.1035	0.0857	0.9999	0.9999
Manual experimentation	/	96.00	70.00	0.1400	0.1000	0.9810	0.9780

Comparing the computational time of MOO models

FlowBO and NEXTorch were ahead of TSEMO in terms of computational speed (Table 6) probably because they were implemented based on the BoTorch framework with GPU acceleration. In addition, the average computational time of FlowBO in these five cases was only 50.6% of that of NEXTorch, which suggests that the qNEHVI[25] algorithm is more computationally efficient than qEHVI[24].

Table 6. Average computational time of the MOO models in each case

Case	Computational time (min)		
	FlowBO	**NEXTorch**	**Summit-TSEMO**
1	0.78	1.98	2.15
2	0.36	2.20	2.28
3	0.78	0.72	1.96
4	0.84	1.32	2.07
5	0.72	0.65	1.88

Discussions

In four of the five cases above, FlowBO performed the best. In Case 4 and Case 5, FlowBO was the only MOO model that achieved >99.9% conversion and selectivity. For the cases where both FlowBO and NEXTorch achieved >99.9% conversion and selectivity, FlowBO provided a larger range of decision variables to choose from, such as temperature and residence time. In some cases, the Top-1 result may not be the best result for the downstream process, such as separation (i.e. the temperature may be too high for separation). Therefore, a range of optimal results with various combinations of variables is preferred, especially for multi-step process optimization[38, 39].

The only case that FlowBO did not perform best was a single-step reaction. A possible reason for the better performance of NEXTorch was that it was more inclined to exploitation. For a single-step reaction, since a suboptimal point may be easier to find, continuous exploitation near that point may be beneficial for further optimization. However, for the other four cases, which are all series reactions, the search space is larger and over-exploitation may trap the search in a local optimum. This may be the

reason why the relatively more exploration-oriented FlowBO performed better in all series reaction cases.

In the case of TSEMO (the version available in Summit), it was difficult to compete with the models with recently-developed acquisition functions because it was developed earlier than EHVI and NEHVI and was not equipped with GPU acceleration. However, as the Lapkin group is actively contributing to the MOO of chemical processes[39, 40], it is likely that more recent versions of TSEMO that could perform better.

A comparison of FlowBO-MOO and FlowBO-SOO in these five cases shows that SOO of yield, while achieving the best optimization results similar to MOO in conversion and selectivity, it typically requires longer residence times (Cases 1 and 3) or higher temperatures (Cases 4 and 5), which leads to higher cost and lower efficiencies. Therefore, when both MOO and SOO are available, MOO should be preferred.

The limitations of this study are as follows. First, only one single-step reaction (Case 2) was included. Although series reactions are more challenging to optimize, more cases of single-step would be beneficial for more comprehensive benchmarking. In addition, the workload was too large to make recommendations from actual experiments as we compared four models under five cases. Therefore, we used kinetic models to simulate the experimental results, as the Lapkin group did in their study of Summit, comparing their TSEMO with other recognized BO models under a benchmark of a kinetic model and a machine learning-based predictive model[21]. However, without conducting real experiments, it is more difficult to introduce real-world noise (although we introduced an error of $\pm 3\%$ for the calculated concentrations) and compare the noise-handling capabilities of the MOO algorithms including NEHVI, EHVI, and TSEMO.

Conclusions

In this work, we presented FlowBO, an open-source Bayesian optimization

framework for optimizing flow chemistry (continuous flow reactions). Since previous studies have rarely compared existing BO frameworks under the benchmark of continuous flow kinetic models, we compared FlowBO with the recently-developed open-source framework NEXTorch and the classical MOO model TSEMO under the benchmark of five kinetic models. FlowBO outperformed NEXTorch in all four series reactions and had a wider choice of decision variables. FlowBO and TSEMO had a wider coverage of the search space and Pareto Front in general, but FlowBO's acquisition function qNEHVI is more efficient than the earlier developed TSEMO.

In the future, we would like to introduce more kinetic model cases, such as more complex single-step reactions and different types of multi-step reactions (i.e. parallel reactions) for a more solid benchmark of the BO models. Meanwhile, we would like to utilize more advanced automated self-optimization platforms equipped with in-line analysis capabilities to better evaluate the capability of the advanced MOO acquisition functions in handling experimental noise.

Conflicts of interest

There are no conflicts of interest to declare.

Acknowledgments

Data Availability Statement

The data and code repository for this study will be made available once the paper is accepted.

References

1.   Ley, S. V.;   Fitzpatrick, D. E.;   Ingham, R. J.; Myers, R. M., Organic synthesis: march of the machines. *Angew Chem Int Ed Engl* **2015,** *54* (11), 3449-64.

2.   Reizman, B. J.; Jensen, K. F., Feedback in Flow for Accelerated Reaction Development. *Acc Chem Res* **2016,** *49* (9), 1786-96.

3.   Shields, B. J.;   Stevens, J.;   Li, J.;   Parasram, M.;   Damani, F.;   Alvarado, J. I. M.;   Janey, J. M.; Adams, R. P.; Doyle, A. G., Bayesian reaction optimization as a tool for chemical synthesis. *Nature* **2021,** *590* (7844), 89-96.

4.   Wei, J. N.;   Duvenaud, D.; Aspuru-Guzik, A., Neural Networks for the Prediction of Organic Chemistry Reactions. *ACS Central Science* **2016,** *2* (10), 725-732.

5.   Movsisyan, M.;   Delbeke, E. I.;   Berton, J. K.;   Battilocchio, C.;   Ley, S. V.; Stevens, C. V., Taming hazardous chemistry by continuous flow technology. *Chem Soc Rev* **2016,** *45* (18), 4892-928.

6.   Negoescu, D. M.;   Frazier, P. I.; Powell, W. B., The Knowledge-Gradient Algorithm for Sequencing Experiments in Drug Discovery. *INFORMS Journal on Computing* **2011,** *23* (3), 346-363.

7.   Larkin, J. P.;   Wehrey, C.;   Boffelli, P.;   Lagraulet, H.;   Lemaitre, G.;   Nedelec, A.; Prat, D., The Synthesis of 17r-Methyl-11â-arylestradiol: Large-Scale Application of the Cerium (III)-Mediated Alkylation of a Ketone. *Organic Process Research & Development* **2002,** *6*, 20-27.

8.   Gotti, R.;   Furlanetto, S.;   Andrisano, V.;   Cavrini, V.; Pinzauti, S., Design of experiments for capillary electrophoretic enantioresolution of salbutamol using dermatan sulfate. *Journal of Chromatography A* **2000,** *875*, 411-422.

9.   den Brok, M. W.;   Nuijen, B.;   Miranda, E.;   Floriano, P.;   Munt, S.;   Manzanares, I.; Beijnen, J. H., Development and validation of a liquid chromatography-ultraviolet absorbance detection assay using derivatisation for the novel marine anticancer agent ES-285 x HCl [(2S,3R)-2-amino-3-octadecanol hydrochloride] and its pharmaceutical dosage form. *J Chromatogr A* **2003,** *1020* (2), 251-8.

10.   Tye, H., Application of statistical 'design of experiments' methods in drug discovery. *Drug Discov Today* **2004,** *9* (11), 485-91.

11.   Snoek, J.;   Larochelle, H.; Adams, R. P., Practical Bayesian Optimization of Machine Learning Algorithms. *NIPS* **2012,** *4*, 2951-2959.

12.   Srinivas, N.;   Krause, A.;   Kakade, S. M.; Seeger, M. W., Information-Theoretic Regret Bounds for Gaussian Process Optimization in the Bandit Setting. *IEEE Transactions on Information Theory* **2012,** *58* (5), 3250-3265.

13.   Shahriari, B.;   Swersky, K.;   Wang, Z.;   Adams, R. P.; de Freitas, N., Taking the Human Out of the Loop: A Review of Bayesian Optimization. *Proceedings of the IEEE* **2016,** *104* (1), 148-175.

14.   Hutter, F.;   Hoos, H. H.; Leyton-Brown, K., Sequential Model-Based Optimization for General Algorithm Configuration. *Internat.Conf. Learn. Intel. Optim.* **2011,** *6683*, 507-523.

15.   snoek, J.;   swersky, K.;   Zemel, R. S.; Adams, R. P., Input Warping for Bayesian Optimization of Non-Stationary Functions, Internat. *Conf.Mach. Learn.* **2014,** *pp*, 1674-1682.

16.   Snoek, J.;   Rippel, O.;   Swersky, K.;   Kiros, R.;   Satish, N.;   Sundaram‡, N.;   Patwary, M. M. A.;   Prabhat; Adams, R. P., Scalable Bayesian Optimization Using Deep Neural Networks. *Internat. Conf. Mach.Learn.* **2015,** *pp*, 2171-2180.

17.   Hase, F.;   Roch, L. M.;   Kreisbeck, C.; Aspuru-Guzik, A., Phoenics: A Bayesian Optimizer for Chemistry. *ACS Cent Sci* **2018,** *4* (9), 1134-1145.

18. Boukouvala, F.; Ierapetritou, M. G., Feasibility analysis of black-box processes using an adaptive sampling Kriging-based method. *Computers & Chemical Engineering* **2012,** *36*, 358-368.

19. Rogers, A.; Ierapetritou, M., Feasibility and flexibility analysis of black-box processes Part 1: Surrogate-based feasibility analysis. *Chemical Engineering Science* **2015,** *137*, 986-1004.

20. Deshwal, A.; Simon, C. M.; Doppa, J. R., Bayesian optimization of nanoporous materials. *Molecular Systems Design & Engineering* **2021,** *6* (12), 1066-1086.

21. Felton, K. C.; Rittig, J. G.; Lapkin, A. A., Summit: Benchmarking Machine Learning Methods for Reaction Optimisation. *Chemistry–Methods* **2021,** *1* (2), 116-122.

22. Bradford, E.; Schweidtmann, A. M.; Lapkin, A., Efficient multiobjective optimization employing Gaussian processes, spectral sampling and a genetic algorithm. *Journal of Global Optimization* **2018,** *71* (2), 407-438.

23. Bradford, E.; Schweidtmann, A. M.; Lapkin, A., Correction to: Efficient multiobjective optimization employing Gaussian processes, spectral sampling and a genetic algorithm. *Journal of Global Optimization* **2018,** *71* (2), 439-440.

24. Daulton, S.; Balandat, M.; Bakshy, E., Differentiable expected hypervolume improvement for parallel multi-objective Bayesian optimization. *Advances in Neural Information Processing Systems* **2020,** *33*, 9851-9864.

25. Daulton, S.; Balandat, M.; Bakshy, E., Parallel bayesian optimization of multiple noisy objectives with expected hypervolume improvement. *Advances in Neural Information Processing Systems* **2021,** *34*, 2187-2200.

26. Schweidtmann, A. M.; Clayton, A. D.; Holmes, N.; Bradford, E.; Bourne, R. A.; Lapkin, A. A., Machine learning meets continuous flow chemistry: Automated optimization towards the Pareto front of multiple objectives. *Chemical Engineering Journal* **2018,** *352*, 277-282.

27. Wang, Y.; Chen, T. Y.; Vlachos, D. G., NEXTorch: A Design and Bayesian Optimization Toolkit for Chemical Sciences and Engineering. *J Chem Inf Model* **2021,** *61* (11), 5312-5319.

28. Balandat, M.; Karrer, B.; Jiang, D.; Daulton, S.; Letham, B.; Wilson, A. G.; Bakshy, E., BoTorch: A framework for efficient Monte-Carlo Bayesian optimization. *Advances in neural information processing systems* **2020,** *33*, 21524-21538.

29. Minasny, B.; McBratney, A. B., A conditioned Latin hypercube method for sampling in the presence of ancillary information. *Computers & Geosciences* **2006,** *32* (9), 1378-1388.

30. ;, A. M. S.; Bongartz;, D.; Grothe;, D.; Kerkenhof;, T.; Lin;, X.; Najman;, J. l.; Mitsos, A., Global optimization of Gaussian processes. *arXiv:2055.10902v1* **2005**.

31. Emmerich, M. T. M.; Giannakoglou, K. C.; Naujoks, B., Single- and multiobjective evolutionary optimization assisted by Gaussian random field metamodels. *IEEE Transactions on Evolutionary Computation* **2006,** *10* (4), 421-439.

32. Jones, D. R., Schonlau, M., and Welch, W. J. , Efficient global optimization of expensive black-box functions. *Journal of Global Optimization* **1998,** *13*, 455-492.

33. Letham, B.; Karrer, B.; Ottoni, G.; Bakshy, E., Constrained Bayesian Optimization with Noisy Experiments. *Bayesian Analysis* **2019,** *14* (2).

34. Xu, Q.; Fan, H.; Yao, H.; Wang, D.; Yu, H.; Chen, B.; Yu, Z.; Su, W., Understanding monoacylation of symmetrical diamines: A kinetic study of acylation reaction of m-phenylenediamine and benzoic anhydride in microreactor. *Chemical Engineering Journal* **2020,** *398*.

35. Xu, Q.; Liu, J. M.; Yao, H.; Zhao, J.; Wang, Z.; Liu, J.; Zhou, J.; Yu, Z.; Su, W., Insight into Fundamental Rules of Phenylenediamines Selective Monoacylation by the Comparisons of Kinetic

Characteristics in Microreactor. *Bulletin of the Korean Chemical Society* **2021,** *42* (10), 1336-1344.

36. Xu, Q.; Zhang, S.; Zhao, J.; Wang, Z.; Liu, L.; Zhou, P.; Yu, Z.; Su, W., Improving the reaction efficiency of condensation amidation of piperazine with benzoic acid based on kinetics study in microreactors. *Journal of Flow Chemistry* **2021,** *11* (4), 855-866.

37. Pedersen, M. J.; Born, S.; Neuenschwander, U.; Skovby, T.; Mealy, M. J.; Kiil, S.; Dam-Johansen, K.; Jensen, K. F., Optimization of Grignard Addition to Esters: Kinetic and Mechanistic Study of Model Phthalide Using Flow Chemistry. *Industrial & Engineering Chemistry Research* **2018,** *57* (14), 4859-4866.

38. Clayton, A. D.; Schweidtmann, A. M.; Clemens, G.; Manson, J. A.; Taylor, C. J.; Niño, C. G.; Chamberlain, T. W.; Kapur, N.; Blacker, A. J.; Lapkin, A. A.; Bourne, R. A., Automated self-optimisation of multi-step reaction and separation processes using machine learning. *Chemical Engineering Journal* **2020,** *384*, 123340.

39. Jorayev, P.; Russo, D.; Tibbetts, J. D.; Schweidtmann, A. M.; Deutsch, P.; Bull, S. D.; Lapkin, A. A., Multi-objective Bayesian optimisation of a two-step synthesis of p-cymene from crude sulphate turpentine. *Chemical Engineering Science* **2022,** *247*, 116938.

40. Pomberger, A.; Pedrina McCarthy, A. A.; Khan, A.; Sung, S.; Taylor, C. J.; Gaunt, M. J.; Colwell, L.; Walz, D.; Lapkin, A. A., The effect of chemical representation on active machine learning towards closed-loop optimization. *Reaction Chemistry & Engineering* **2022,** *7* (6), 1368-1379.